Glycoconj J (2013) 30:781–789
DOI 10.1007/s10719-013-9482-x

Altered expression of *O*-GlcNAc-modified proteins in a mouse model whose glycemic status is controlled by a low carbohydrate ketogenic diet

Tetsuya Okuda · Asami Fukui · Naoki Morita

Received: 16 April 2013 / Revised: 23 May 2013 / Accepted: 27 May 2013 / Published online: 21 June 2013

Abstract Abnormal modification of proteins by *O*-linked *N*-acetylglucosamine (*O*-GlcNAc) is known to be associated with the pathology induced by hyperglycemia. However, the dynamic mechanism of *O*-GlcNAc modification under hyperglycemic conditions *in vivo* has not been fully characterized. To understand the mechanism, we established an animal model in which the glycemic status is controlled by the diet. A mutant mouse (*ob/ob*) which exhibits diet-induced hyperglycemia when fed a regular chow (chow) was used to establish this model; the mice were fed a very low carbohydrate ketogenic diet (KD) to improve hyperglycemia. Using this model, we evaluated the levels of *O*-GlcNAc-modified proteins in tissues under a hyperglycemic or its improved condition. ELISA and Western blot analyses revealed that altered expression of certain proteins modified by *O*-GlcNAc were found in the mice tissues, although global *O*-GlcNAc levels in the tissues remained unaltered by improvement of hyperglycemia. We also found the Akt protein kinase was modified by *O*-GlcNAc in the liver of *ob/ob* mice, and the modification levels were decreased by improvement of hyperglycemia. Furthermore, aberrant phosphorylation of Akt was found in the liver of *ob/ob* mice under hyperglycemic condition. In conclusion, our established mouse model is useful for evaluating the dynamics of *O*-GlcNAc-modified proteins in tissues associated with glycemic status. This study revealed that the expression level of certain proteins modified by *O*-GlcNAc is altered when KD improves the hyperglycemia. These proteins could be prospective indexes for nutritional therapy for hyperglycemia-associated diseases, such as diabetes mellitus.

Keywords Diabetes mellitus · Hyperglycemia · Ketogenic diet · Obese mice · *O*-GlcNAc · *O*-GlcNAcase · *O*-GlcNAc transferase

Introduction

The *O*-linked *N*-acetylglucosamine (*O*-GlcNAc) modification on proteins is a posttranslational modification, occurring on cytoplasmic and nuclear proteins in which a single *O*-linked *N*-acetylglucosamine residue attaches to serine or threonine moieties [1]. There are two key enzymes catalyzing *O*-GlcNAc modification: *O*-GlcNAc transferase (OGT) and *O*-GlcNAcase (OGA). OGT transfers GlcNAc from UDP-GlcNAc to a protein, and OGA removes the GlcNAc residue from that protein [2, 3]. This reversible modification regulates a variety of cellular processes, such as transcription, signal transduction, protein trafficking and turnover [4, 5]. *O*-GlcNAc modification and phosphorylation of serine and threonine moieties are considered to be linked and play an important role in cellular processes.

Recent reports revealed that abnormal *O*-GlcNAc modification of proteins is associated with several pathologies exhibiting hyperglycemia, a typical disease of which is diabetes mellitus [6]. Numerous studies have addressed the role of proteins modified by *O*-GlcNAc on the molecular basis of the pathology of diabetes mellitus, including insulin resistance [6–8] and glucose intolerance [6, 9]. For example, the *O*-GlcNAc modification affects phosphorylation status of Akt protein kinase that is related to insulin signaling. Enhanced *O*-GlcNAc modification of Akt induced by chemical treatment

Electronic supplementary material The online version of this article (doi:10.1007/s10719-013-9482-x) contains supplementary material, which is available to authorized users.

T. Okuda (✉) · A. Fukui · N. Morita
Molecular and Biological Technology Research Group, Bioproduction Research Institute, National Institute of Advanced Industrial Science and Technology (AIST), 2-17-2-1 Tsukisamu-higashi, Toyohira-ku, Sapporo 062-8517, Japan
e-mail: t-okuda@aist.go.jp

or overexpression of OGT decrease phosphorylation level of Akt at Thr 308 that is necessary for the activation of insulin signaling pathway [8, 10].

UDP-GlcNAc, the donor of *O*-GlcNAc, is synthesized from glucose in the cell *via* the hexosamine biosynthetic pathway (HBP) [6]. Thus, a hyperglycemic condition is expected to influence the levels of *O*-GlcNAc modification of intracellular proteins. However, neither intracellular levels of glucose nor the kinetics of catabolic enzymes for *O*-GlcNAc are simply reflected in the levels of proteins modified by *O*-GlcNAc. These levels are intricately regulated under various cellular processes that include the altered expression of OGT and OGA [11–15]. Therefore, the molecular dynamics of *O*-GlcNAc modification and its modified proteins under physiological conditions remains elusive.

Several animal models whose glycemic status controlled surgically [16] or pharmacologically [16–18] have been used to evaluate the molecular dynamics of the *O*-GlcNAc modification *in vivo*. Type 1 diabetic rodent models are frequently used for the purpose of this evaluation, however, diabetes is induced by Streptozotocin injection which has an inhibitory effect on the cleavage of *O*-GlcNAc from proteins, leading to the accumulation of *O*-GlcNAc proteins in cells without hyperglycemia [19, 20]. To understand the molecular dynamics of the *O*-GlcNAc modification and its pathological role, it is necessary to establish an animal model that closely reflects the physiological conditions and lifestyle of hyperglycemic patients.

We have recently reported an animal model of which the glycemic status is controlled by diets [21]. An obese mutant mouse strain B6.V-Lep^{ob}/J (*ob/ob*) that exhibits diet-induced hyperglycemia [22] was used to develop the model. The *ob/ob* mouse exhibits hyperphagia with development of obesity, steatosis, hyperinsulinemia and hyperglycemia after being fed a diet of regular chow (chow). We determined an optimal condition to improve the hyperglycemic phenotype of *ob/ob* mice by feeding a very low carbohydrate ketogenic diet (KD). KD is theoretically a nutritionally balanced diet, composed of high fat, adequate protein and low carbohydrate [21, 23]. The KD mimics glucose starvation in the body, leading to production of ketone bodies from fat, which supplies energy to peripheral tissues [21, 23, 24]. By using this model, we revealed the KD feeding could improve hyperglycemia, hyperinsulinemia and hepatic steatosis in *ob/ob* mice [21].

In this report, we describe the molecular dynamics of the *O*-GlcNAc-modified proteins in the mice model. Evaluation of the expression levels of *O*-GlcNAc-modified proteins, its catabolic enzymes, and phosphorylation status of Akt in mice tissues revealed the molecular dynamics of protein *O*-GlcNAc modification in tissues under hyperglycemia.

Materials and methods

Animals and dietary studies

All mice used in this study were female wild-type and *ob/ob* mutant mice of the inbred strain C57BL/6 (Charles River Laboratories Japan, Yokohama, Japan). Mice were maintained with a 12 h-light/dark cycle in a temperature-controlled environment (21 °C±2 °C). CE-2 (CLEA Japan, Tokyo, Japan) and F3666 (Bio-Serv, Frenchtown, NJ) were used as regular chow and KD, respectively. The components of these diets are described in Table 1. Five-week-old *ob/ob* mice were raised on either chow or KD until 12 weeks old. Wild-type mice raised on chow and the same experimental conditions were used as a reference. During this period, body weight and blood glucose levels were monitored at the same time (3:00 p.m.) once a week. The Committee for Experiments involving Animals of the National Institute of Advanced Industrial Science and Technology (AIST) approved all animal experiments.

Blood chemical analysis

Blood glucose levels were examined using venous blood collected from the tail vain and the ACCU-CHEK™ Aviva meter system (Roche, Penzberg, Germany). Serum insulin levels were measured with the Mouse Insulin ELISA Kit High Range Speedy (Morinaga Institute of Biological Science, Yokohama, Japan).

Preparation of protein extracts

Proteins were extracted from each isolated tissue (80 mg in weight) into 0.4 ml of 20 mM HEPES/0.25 M sucrose buffer (pH 7.5) supplemented with 0.1 mM phenylmethylsulfonyl fluoride, a proteinase inhibitor cocktail (Complete mini

Table 1 Composition of the experimental diets[a]

Ingredient	CE-2	KD
Content profile (%)		
Carbohydrate	50.0	3.2
Fat	4.8	78.8
Protein	25.1	8.4
Fiber	4.2	5.0
Ash	6.7	3.8
Moisture	9.3	<5.0
Caloric profile (Kcal/g)		
Carbohydrate	2.00	0.13
Fat	0.43	7.09
Protein	1.00	0.33
Total	3.43	7.55

[a] The profiles of principle contents in the experimental diets are shown

EDTA-free™; Roche) and 2 μM of an OGA inhibitor *O*-(2-acetamido-2-deoxy-D-glucopyranosylidene)amino *N*-phenylcarbamate (PugNAc; Toronto Research Chemicals, North York, ON) using a disposable homogenizer (Biomasher II; Nippi, Tokyo, Japan). After centrifugation of the homogenates at 800 × *g* for 15 min at 4 °C, the supernatants were filtered using an Ultrafree-MC (0.45 μm) centrifugal device (Millipore, Billerica, MA) at 13,000 × *g* for 3 min at 4 °C. The filtrates were used as protein samples in subsequent experiments. The concentration of protein in the sample was determined using the Bio-Rad Protein Assay (Bio-Rad Laboratories, Hercules, CA).

Enzyme-linked immunosorbent assay (ELISA)

50 μl of protein extracts (final concentration 20 μg/ml) were applied onto a 96-well microtiter plate (Nunc MaxiSorp F96; Thermo Fisher Scientific, Waltham, MA), and incubated overnight at 4 °C. After washing twice with phosphate buffered saline (PBS), 50 μl of blocking buffer (1 % bovine serum albumin in PBS) were added into each well and incubated for 15 min at room temperature, followed by the addition of primary antibodies into the wells at an appropriate dilution ratio. After 3 h incubation at room temperature, wells were washed three times with 0.1 % Tween-20 in PBS (PBST) before PBST-diluted HRP-linked secondary antibody was added. A HRP substrate (1-Step Ultra TMB-ELISA Substrate; Thermo Fisher Scientific) was used to detect antibody binding, and the results were measured as absorbance at 450 nm. Wells without the primary antibody reaction were used to monitor background absorbance caused by non-specific binding of secondary antibody. Primary antibodies used were: anti-*O*-GlcNAc (CTD110.6; Sigma-Aldrich, St. Louis, MO), anti-OGT (SAB2500715; Sigma-Aldrich), anti-OGA (EPR7154B; Epitomics, Burlingame, CA) and anti-actin (C4; BD Biosciences, Franklin Lakes, NJ). The range of linearity and detection limit of the ELISA were determined using a protein extract of human umbilical vein endothelial cells in which the *O*-GlcNAc protein excessively accumulated after treatment of 50 μM PugNAc for 16 h.

SDS-PAGE and Western blotting

Protein extracts containing 2 μg (fat tissue) or 5 μg (other tissues) of total protein were separated by sodium dodecyl sulfate-polyacrylamide gel electrophoresis (SDS-PAGE) using a polyacrylamide gel (SuperSep™ 5–20 % Gel; Wako chemicals, Osaka, Japan); the gel was stained with Coomassie Brilliant Blue (CBB) or used in Western blotting. For Western blotting, the proteins in the gel were transferred onto Immobilon-P PVDF membranes (Millipore) by electroblotting at a constant current of 90 mA for 1 h. After blotting, the membrane was incubated with primary antibody, and then sequentially incubated with HPR-linked secondary antibody. Antibody binding was detected using ECL Plus Western Blotting Detection Reagents (GE Healthcare UK Ltd., Amersham, UK) and an image analyzer: ATTO Light-Capture (ATTO, Tokyo, Japan). Primary antibodies used were: anti-*O*-GlcNAc (CTD110.6 or RL2; Thermo Fisher Scientific), anti-OGT (SAB2500715), anti-OGA (EPR7154B), anti-Akt (#9272; Cell Signaling Technology, Danvers, MA), anti-phospho-Akt-Ser 473 (#9271; Cell Signaling Technology) and anti-phospho-Akt-Thr 308 (#9275; Cell Signaling Technology).

Immunoprecipitation

Protein extracts containing 2 mg of total protein were incubated with 8 μg of primary antibody at 4 °C overnight, and then incubated with 20 μl of 50 % Protein A Sepharose bead slurry (GE Healthcare, Piscataway, NJ) at 4 °C for 3 h. The samples were centrifuged at 14,000 × *g* for 1 min at 4 °C, and the precipitates (beads) were washed five times with 0.5 ml of Wash Buffer (20 mM Tris–HCl pH 7.5, 150 mM NaCl, 1 mM EDTA, 1 mM EGTA, 1 % Triton X-100, 2.5 mM sodium pyrophosphate, 1 mM β-glycerophosphate, 1 mM Na_3VO_4, 1 μg/ml Leupeptin, 1 mM phenylmethylsulfonyl fluoride, 50 μM PugNAc), and were finally resuspended in 20 μl of SDS-PAGE sample buffer (Wako chemicals). The precipitated proteins were used for Western blot analysis. For the immunoprecipitation, anti-Akt antibody (Cell Signaling Technology) was used as primary antibody. For the blot analysis of immunoprecipitates, the anti-Akt antibody (Cell Signaling Technology) and anti-*O*-GlcNAc antibody (RL2) were used.

Statistical analysis

Statistical significance was determined using Student's *t*-test, taking the case of $*P<0.05$, $**P<0.01$, $***P<0.001$ as statistically significance.

Results

Effect of KD feeding on glycemic status, body weight and serum insulin levels in the established animal model

An obese mutant mouse with the C57BL/6 genetic background (*ob/ob*) is rapidly exhibits a hyperglycemic phenotype after weaning, although the phenotype subsides around 14 weeks of age [22]. We have recently developed an animal model that the hyperglycemic phenotype of *ob/ob* mice is improved by feeding of KD [21]. Five-week-old mice were used in this experiment and were fed by chow or KD until 12 weeks old. In the model, the chronic hyperglycemic phenotype of *ob/ob* mice is improved by feeding KD through the experimental period.

First, we confirmed the hyperglycemic phenotype of the *ob/ob* mice when fed a regular chow (CE-2). The profiles of principle contents of CE-2 are shown in Table 1. We confirmed that chow-fed *ob/ob* mice continuously exhibited high levels of blood glucose from 5 to 12 weeks of age in this experiment (Supplemental Fig. S1a). The average blood glucose level during the experimental period of chow-fed *ob/ob* mice was 194.6 mg/dl. Constitutive hyperphagia with development of obesity, which is a major phenotype of chow-fed *ob/ob* mice, was associated with the hyperglycemic phenotype. Next, we confirmed whether KD would improve the chronic hyperglycemic phenotype. The profiles of principle contents of KD are shown in Table 1. While feeding KD, *ob/ob* mice exhibited lower blood glucose levels than those of chow-fed *ob/ob* mice (Supplemental Fig. S1a). The average blood glucose level during the experimental period of KD-fed *ob/ob* mice was 103.6 mg/dl. The levels of blood glucose in chow-fed wild-type mice (c57BL/6), under the same experimental conditions was 142.4 mg/dl (data not shown), thus, the levels in KD-fed *ob/ob* mice were lower than in chow-fed wild-type mice. However, the KD-fed *ob/ob* mice grew up without apparent abnormalities during the experimental period. They exhibited an obese phenotype at the same time as chow-fed *ob/ob* mice (Supplemental Fig. S1b), and there were no differences in the calorific intake (kcal/day) between both groups (data not shown). The KD-fed *ob/ob* mice also exhibited lower blood levels of insulin compared to chow-fed *ob/ob* mice (Supplemental Fig. S1c). Other details of the KD effects including biochemical parameters in serum and pathology of tissues were published elsewhere [21]. We isolated tissue samples from both chow- and KD-fed *ob/ob* mice at the endpoint of the feeding experiment (12 weeks of age) for use in the experiments described below.

Analysis of protein *O*-GlcNAc modification by ELISA

A monoclonal antibody (CTD110.6) which specifically recognizes the β-*O*-linkage of GlcNAc to both serine and threonine [25] was used in this analysis. We preliminarily examined the detection range of the ELISA (Fig. 1a) using cell extracts in which *O*-GlcNAc-modified proteins accumulated after treatment with a potent inhibitor for OGA, described in Materials and methods. The result indicated that the ELISA reaction showed linearity in coated wells with protein extracts in the range of 0.5 to 20 μg/ml. Because the expression levels of *O*-GlcNAc-modified proteins in the tissue extracts were expected to be lower than in the cell extracts, which were treated with OGA inhibitor, we performed the following ELISA analysis using protein extracts at the maximum concentration determined (20 μg/ml). We also used ELISA to determine the relative content of actin in each protein extract (Fig. 1c): the determined levels were used as an internal control for normalization of ELISA analysis (Figs. 1b and 2a, b).

We found that *O*-GlcNAc levels in each protein extract differed according to the tissue extract examined (Fig. 1b): *O*-GlcNAc was detected at a high level in liver and pancreas, at a moderate level in kidney and levels were relatively low

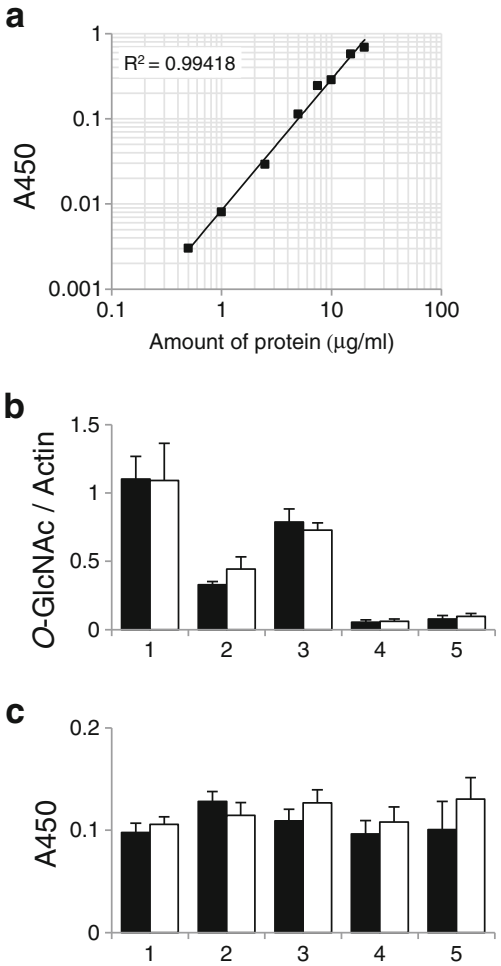

Fig. 1 ELISA analysis of *O*-GlcNAc-modified proteins in tissues from established mice. **a** Reactivity of anti-*O*-GlcNAc monoclonal antibody (CTD110.6) to determine the concentration of *O*-GlcNAc-modified proteins in cellular extracts. A cellular protein extract in which *O*-GlcNAc-modified proteins accumulated with treatment of an OGA inhibitor (PugNAc) was used in this assay. The extract was coated onto each well of a 96-well microtiter plate at the indicated protein concentrations (*horizontal axis*). The reactivity of anti-*O*-GlcNAc monoclonal antibody (CTD110.6) to the coated wells was measured by ELISA, and the results (absorbance at 450 nm) are as indicated (A450). The data is displayed as a double logarithmic graph. The regression line and the correlation coefficient (R^2) are indicated in the *graph*. The global *O*-GlcNAc levels (**b**) and relative content of actin (A450) (**c**) in protein extracts of individual tissues determined by ELISA. These global *O*-GlcNAc levels in each tissue were normalized with respect to the relative content of actin in each protein extract and the relative levels (*O*-GlcNAc/Actin) were determined. *Closed bars*; chow-fed *ob/ob* mice, *open bars*; KD-fed *ob/ob* mice. *1*, liver; *2*, kidney; *3*, pancreas; *4*, skeletal muscle; *5*, fat tissue. *Error bars*: mean ± S.D., *n*=9 (liver, kidney, pancreas) or 5 (skeletal muscle, fat tissue) from two independent experiments

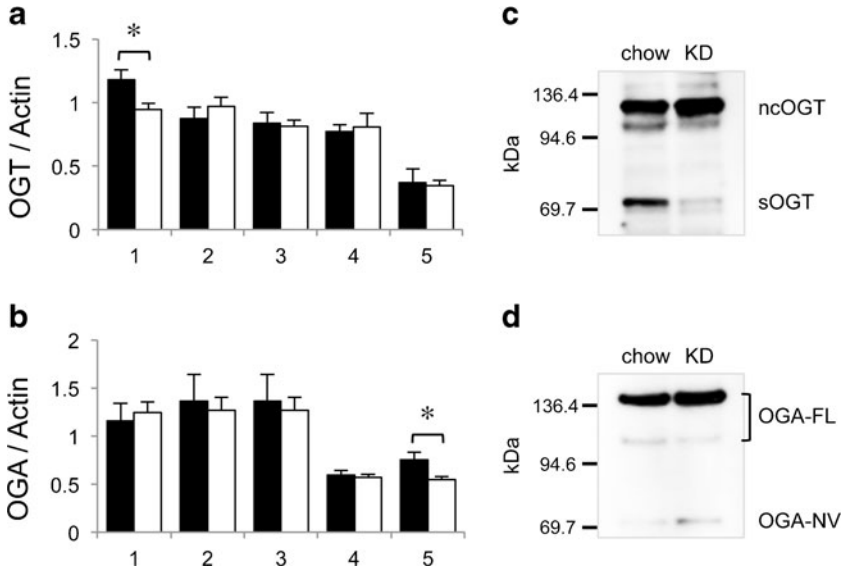

Fig. 2 ELISA and Western blot analysis of OGT and OGA in tissues from established mice. The OGT (**a**) and OGA (**b**) levels in protein extracts of individual tissues from chow-fed (*closed bars*) or KD-fed (*open bars*) *ob/ob* mice determined by ELISA. These levels in each tissue were normalized with respect to the relative content of actin in each protein extract and the relative levels (OGT/Actin, OGA/Actin) were determined. *1*, liver; *2*, kidney; *3*, pancreas; *4*, skeletal muscle; *5*, fat tissue. Error bars: mean ± S.D., $n=9$ (liver, kidney, pancreas) or 5 (skeletal muscle, fat tissue) from two independent experiments. *$P<0.05$, chow-fed *ob/ob* mice *vs.* KD-fed *ob/ob* mice. **c**, **d** Pooled samples of individual liver (**c**) and fat (**d**) extracts of chow-fed (chow) and KD-fed *ob/ob* mice (KD) were separated by SDS-PAGE, and were immunoblotted with anti-OGT antibody (**c**) or anti-OGA antibody (**d**) respectively. ncOGT; nucleocytoplasmic OGT, sOGT; shortest form of OGT, OGA-FL; cytosolic full-length form of OGA, OGA-NV; nuclear variant of OGA

in skeletal muscle and fat tissue (intra-abdominal fat). We then examined the correlation between blood glucose and *O*-GlcNAc levels in these tissues by comparing chow- or KD-fed *ob/ob* mice groups: no significant differences were determined.

ELISA and Western blot analysis of OGT and OGA

Next, we analyzed the relative contents of OGT and OGA in these tissues of the established mouse model using ELISA (Fig. 2a, b). It is reported that OGT and OGA are not only the key enzymes for biosynthesis of *O*-GlcNAc [2, 3] but also the substrates for *O*-GlcNAc modification [26, 27]. We found significant differences in these relative contents in the liver and fat tissue between the chow- and KD-fed *ob/ob* mice groups; in *ob/ob* mice, KD feeding decreased the expression levels of OGT in liver (Fig. 2a) and OGA in fat tissue (Fig. 2b).

We further analyzed the isoform variation of OGT and OGA in these tissues by Western blotting (Fig. 2c, d). The Western blot analysis of OGT in liver revealed that two major isoforms of OGT were detected in the *ob/ob* mice liver (Fig. 2c). The isoform detected in the high molecular weight is known as nucleocytoplasmic OGT (ncOGT), and the other is known as shortest form of OGT (sOGT) [28, 29]. The result indicated that only sOGT was markedly decreased in the KD-fed *ob/ob* mice liver. Previous studies reveal that OGA has two isoforms, cytosolic full-length form (OGA-FL) and nuclear variant (OGA-NV) [29, 30]. The OGA-FL is also known to be detected as double bands in rat brain [29]. In the fat tissue, OGA was predominantly detected as OGA-FL single band, and other isoforms were hardly detected (Fig. 2d).

Western blot analysis of *O*-GlcNAc-modified proteins in the liver of *ob/ob* mice

The expression levels of *O*-GlcNAc-modified proteins in the liver was further analyzed by Western blotting after SDS-PAGE, and we compared the results between chow- and KD-fed *ob/ob* mice. First, we analyzed the protein extracts by SDS-PAGE combined with CBB staining and revealed that altered expressions of protein bands were observed in the liver of KD-fed *ob/ob* mice (Fig. 3a). Although the protein bands in the chow-fed *ob/ob* mice group were almost similar in expression intensity to those in the KD-fed *ob/ob* mice group, the intensity of several bands, especially band highlighted with arrowhead, is decreased in KD-fed *ob/ob* mice group. This result indicates that KD feeding alters the expression levels of a part of proteins in *ob/ob* mice.

Next we used CTD110.6 antibody and detected six protein bands at a high intensity in the liver of chow-fed group (Fig. 3b; arrows I–VI). Of the six intense bands of proteins, the band highlighted with arrow II and VI, in Fig. 3b, were detected at reduced levels in the KD-fed group. Image analysis revealed that the intensity of band II and VI in the KD-fed

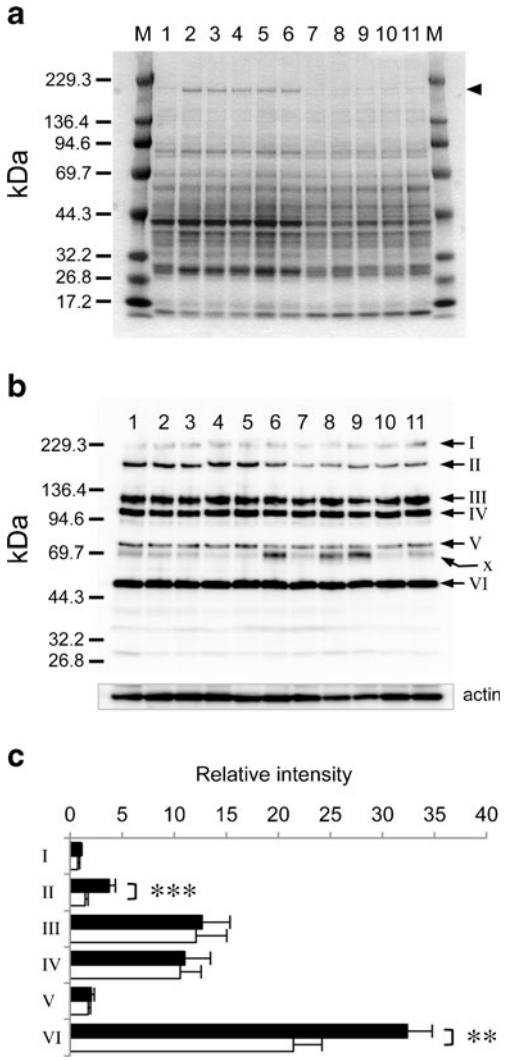

Fig. 3 Western blot analysis of *O*-GlcNAc-modified proteins in liver. Individual liver extracts of chow-fed (*lanes 2–6*) and KD-fed *ob/ob* mice (*lanes 7–11*) were separated by SDS-PAGE, and stained with CBB (**a**) or analyzed by Western blotting (**b**). Liver extract from a chow-fed wild-type mouse (*lane 1*) was loaded as a reference. The *arrowhead* in (**a**) highlighted a protein band in which different expression was observed between chow and KD-fed *ob/ob* mice. *Arrows* (I–VI) in (**b**) were highlighted major protein bands detected by anti-*O*-GlcNAc antibody. The band highlighted by *arrow x* is immunoglobulin-μ chain which was detected as background by the secondary antibody reaction. The *lower panel* in (**b**) indicated the result of Western blotting of actin contents in the extracts. **c** The intensities of major bands detected by Western blotting (*arrows* in **b**, I–VI) were analyzed using an image analyzer and are represented as relative intensity. *Error bars*: mean ± S.E., $n=9$ from two independent experiments. $^{**}P<0.01$, $^{***}P<0.001$ chow-fed *ob/ob* mice *vs.* KD-fed *ob/ob* mice

group was significantly lower (II, $P<0.001$; VI, $P<0.01$) than that in the chow-fed group (Fig. 3c). Other bands showed no significant difference between the two groups (Fig. 3b, arrows I, III–V). Such reduced level of *O*-GlcNAc protein in the liver was also detected by the other anti-*O*-GlcNAc antibody (RL2) whose specificity is different from CTD110.6 antibody [31, 32]. The Western blot analysis of liver extracts using RL2 antibody showed a different detection pattern to the pattern using CTD110.6 antibody (Supplemental Fig. S2a). The RL2 antibody detected some intense bands, and we found that the expression level of one of them was significantly lower in KD-fed group than chow-fed group (Fig. S2b).

We also analyzed the expression patterns of *O*-GlcNAc-modified proteins in kidney, pancreas, skeletal muscle, and fat tissue of *ob/ob* mice (Supplemental Figs. S3, S4), and found several bands which alter the expression levels by KD feeding. The analysis was performed with CTD 110.6 antibody. In pancreas and skeletal muscle, we found two protein bands (Fig. S3e, arrow IV; Fig. S4b, arrow IV) that the expression levels are decreased by KD feeding ($p<0.05$). In contrast, we found two bands that are increased in kidney (Fig. S3b, arrow IV) and fat tissue (Fig. S4e, arrow III) by KD feeding ($p<0.05$).

Western blot analysis of *O*-GlcNAc-modified Akt proteins in the liver of *ob/ob* mice

Because of the drastic decrease of serum insulin of the KD-fed *ob/ob* mice, (Supplemental Fig. 1c,), it was considered that the KD feeding has some effect on insulin signaling. Specifically, we investigated a phosphorylation status of Akt protein kinase in the liver of both chow-fed and KD-fed *ob/ob* mice by Western blotting. It is known that phosphorylation level of Akt at Ser 473 and Thr 308 are enhanced by insulin stimulation and required for the activation of insulin signaling pathway in the cell [33]. As expected, the phosphorylation level of Akt at Ser 473 in chow-fed *ob/ob* mice was significantly higher than that of KD-fed *ob/ob* mice (Fig. 4b, d) due to the high level of serum insulin. However, there was no difference in the levels of phosphorylation of Akt at Thr 308 between two groups (Fig. 4b, c). The result indicates that the enhancement of Thr 308 phosphorylation of Akt by high serum insulin is disturbed in the liver of chow-fed *ob/ob* mice. Because the Akt Thr 308 phosphorylation is known to be attenuated by *O*-GlcNAc modification of Akt protein [8, 10, 34], we investigated the *O*-GlcNAc modification of Akt protein in the both of *ob/ob* mice group. We conducted Western blotting for the *O*-GlcNAc-modified protein which is immunoprecipitated by anti-Akt antibody. RL2 antibody was used in this assay because the *O*-GlcNAc-modified Akt was not detected by the CTD110.6 antibody. As a result, the Akt protein in chow-fed *ob/ob* mice is modified by *O*-GlcNAc, and the modification level is decreased by KD feeding (Fig. 4a).

Discussion

We have recently reported a mouse model in which the glycemic status is controlled by feeding a regular or a low

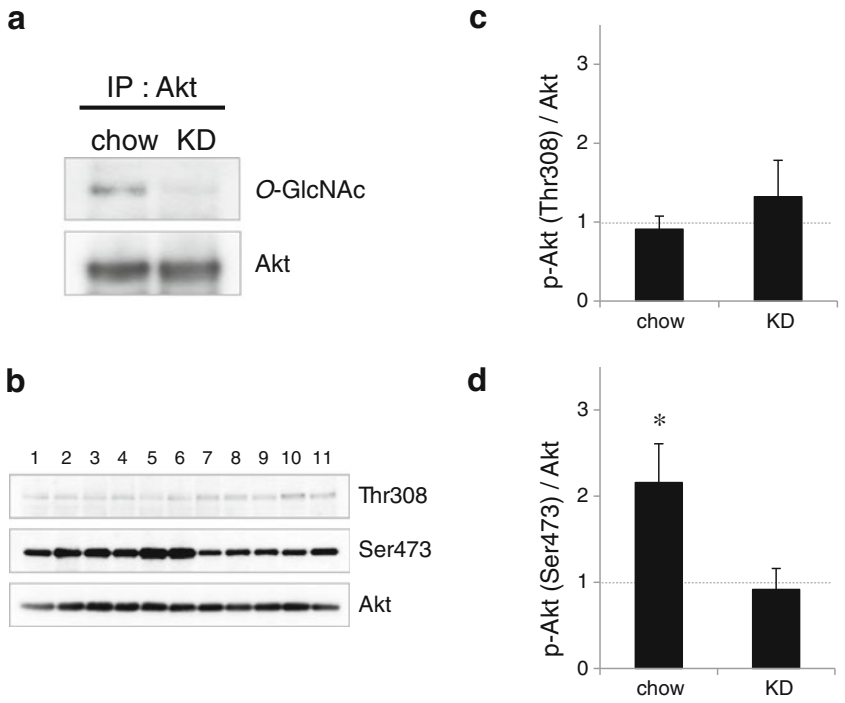

Fig. 4 Immunoprecipitation analysis of *O*-GlcNAc modification of the Akt protein kinase in liver. **a** Pooled samples of individual liver extracts of chow-fed (chow) and KD-fed (KD) *ob/ob* mice were immunoprecipitated with anti-Akt antibody, and the precipitated proteins were immunoblotted with anti-*O*-GlcNAc antibody (*upper panel*) or anti-Akt antibody (*lower panel*). **b** Individual liver extracts of chow-fed (*lanes 2–6*) and KD-fed *ob/ob* mice (*lanes 7–11*) were separated by SDS-PAGE, and were immunoblotted with anti-Phospho-Akt-Thr 308 antibody (*upper panel*), anti-Phospho-Akt-Ser 473 antibody (*middle panel*) and anti-Akt antibody (*lower panel*), respectively. The intensities of phosphorylated bands of Thr 308 (**c**) and Ser 473 (**d**) of chow-fed (chow) and KD-fed *ob/ob* (KD) mice were analyzed using an image analyzer, and were first normalized with respect to the intensity of the band of chow-fed wild-type mice (**b**, *lane 1*), and then the relative levels (p-Akt/Akt) were determined. *Error bars*: mean ± S.D., $n=5$. *$P<0.05$ chow-fed *ob/ob* mice *vs.* KD-fed *ob/ob* mice

carbohydrate ketogenic diet [21]. Because it is known that *ob/ob* mutant mice with the C57BL/6 genetic background exhibit a marked hyperglycemic phenotype in their juvenile stage [22], we focused on this phenotype and succeeded in developing the above animal model. Because the KD feeding could restrict the intake of glucose by diet, the hyperglycemia of *ob/ob* mice, which is initiated by hyperphagia, is improved by KD feeding. The improvement of hyperglycemia also reduces insulin secretion of pancreatic beta cells, and result in the improvement of hyperinsulinemia of *ob/ob* mice (Supplemental Fig. S1c). Using regular chow (CE-2) feeding, hyperglycemia was confirmed in the *ob/ob* mice, and the average level of blood glucose during the experimental period (5 to 12 weeks old) was 194.6 mg/dl. KD feeding improved the hyperglycemic phenotype of *ob/ob* mice: the average level of blood glucose was 103.6 mg/dl. The glycemic status of each group was maintained during the experimental period (Supplemental Fig. S1a), indicating the phenotype was developed chronically. Because the level of blood glucose in the chow-fed wild type mice was 142.4 mg/dl (data not shown), the levels in chow- or KD-fed *ob/ob* mice were obviously high or low, respectively, compared with wild-type mice. The levels of blood glucose in chow- or KD-fed *ob/ob* mice were nearly identical to the levels in type 2 diabetes patients and normal subjects, respectively [15].

Some reports indicate that hyperglycemia is affected to the expression levels of *O*-GlcNAc-modified proteins that are associated with the pathologies of diabetes such as insulin resistance [6–8]. In this study, we examined the relationship between hyperglycemia and the protein *O*-GlcNAc modification by using the established model. The results of ELISA analysis revealed that the global *O*-GlcNAc levels in tissues of *ob/ob* mice were strictly maintained at a constant level (Fig. 1b), in spite of hyperglycemia or its improved condition. However, we also found the altered expression of certain *O*-GlcNAc-modified protein bands in the tissue lysates of KD-fed *ob/ob* mice using Western blot analysis (Figs. 3, S2, S3, S4). These results agree with a recent study which analyzed the erythrocyte proteins from diabetic and normal individuals [35]. This study disclosed that among the many erythrocyte proteins modified by *O*-GlcNAc, only *O*-GlcNAc modification of certain erythrocyte proteins reflected the glycemic status of individuals. The observation supports our conclusion that the dynamics of *O*-GlcNAc modification found in our established mouse model is due to changes in their glycemic status.

Although the regulatory mechanism of altered expression of the *O*-GlcNAc-modified protein observed in the KD-fed *ob/ob* mice remains unclear, this study provided valuable information about the mechanism. In the liver, a decreased expression of OGT, especially sOGT isoform, was found in the *ob/ob* mice after being fed KD (Fig. 2c). Previous report shows that sOGT retains a potentially active catalytic domain, but not the ability to glycosylate substrate proteins that are glycosylated by other OGT isoforms [27]. The substrate specificity of sOGT might be involved in the altered expression of certain *O*-GlcNAc proteins (Fig. 3b, arrow II and VI) in the KD-fed *ob/ob* mice. In the fat tissue, we found decreased expression of OGA (Fig. 2b) and enhanced expression of an *O*-GlcNAc modified protein (Fig. S4e, arrow III) in the *ob/ob* mice after being fed KD. Western blot analysis revealed that a single isoform of OGA (OGA-FL) was predominantly expressed in the fat tissue (Fig. 2d). Because isoform variations are not observed, the OGA-FL plays an important role in the regulation of *O*-GlcNAc modified proteins in fat tissue. We consider that the alteration of OGA-FL kinetics to substrate proteins leads to such specific increase of *O*-GlcNAc proteins. Protein analysis revealed that improvement of hyperglycemia reduces not only the expression levels of OGT and OGA but also the expression levels of several proteins in the *ob/ob* mice tissues (Fig. 3a, S3d, S4d, arrowheads). The results suggested that the decreased expression of the *O*-GlcNAc-modified protein might be partly due to the decreased expression of its core protein.

In this study, we found a protein modified by *O*-GlcNAc that is markedly decreased in the *ob/ob* mice liver by KD feeding (Fig. 3b, arrow II). The protein property might be a prospective index for nutritional therapy for hyperglycemia-associated diseases. Although we have examined to identify the *O*-GlcNAc-modified protein but we failed to identify the protein substrate. Further investigation using our established mouse model will help to identify the protein, and clarify the ability as a marker for hyperglycemia-associated diseases.

Immunoprecipitation analysis revealed that Akt protein kinase is modified by *O*-GlcNAc in the liver of *ob/ob* mice, and the modification level is decreased by improvement of hyperglycemia. The *O*-GlcNAc modification of Akt was known to be increased by treatment of OGA inhibitor (PugNAc) or overexpression of OGT [8, 10, 34, 36]. Our results demonstrated that the modification is also increased by hyperglycemia *in vivo*. We also found a disturbance of the phosphorylation of Akt at Thr 308 in the liver under hyperglycemia. It is known that the two phosphorylations (at Ser 473 and Thr 308 of Akt), which are enhanced by insulin stimulation, are required for the full activation of Akt and insulin signaling pathway in the cell [33]. Thus, it is considered reasonable that the phosphorylation level of both Akt Ser 473 and Akt Thr 308 will be increased in the chow-fed mice, because of the high serum insulin level in these mice (Fig. S1c). However, no increase in the phosphorylation level of Akt Thr 308 of chow-fed mice was observed compared to KD-fed mice, whereas the phosphorylation level of Ser 473 was significantly higher in chow-fed mice than KD-fed mice (Fig. 4c, d). Because it has been reported that *O*-GlcNAc modification of Akt attenuated the phosphorylation levels of Akt at Thr 308 but not at Ser 473 [8], the disturbance of Akt Thr 308 phosphorylation should be due to the high level of *O*-GlcNAc modification on Akt. This phenotype might be related to insulin resistance that is observed in the patients of diabetes mellitus. The phosphorylation and *O*-GlcNAc modification of Akt are dynamically regulated at the phosphoinositide-containing membrane domain in the cell [8]. Like Akt, OGT has phosphoinositide-binding domain, and the domain locates at the C-terminal region of OGT. Insulin stimulation promotes the phosphoinositide-mediated interaction of Akt and OGT, and then enhances the *O*-GlcNAc modification of Akt. Because sOGT retains the phosphoinositide-binding domain [37] and increases the expression level in chow-fed *ob/ob* mice liver, this OGT isoform might promote the *O*-GlcNAc modification of Akt under hyperglycemic condition.

Our study also showed that KD feeding improves not only hyperglycemia but also hyperinsulinemia in the *ob/ob* mice. It is reported that activation of insulin signaling pathway in cells could also enhance the *O*-GlcNAc modification of Akt [36]. They showed that the activation of insulin signaling pathway by insulin-like growth factor 1 (IGF-1) stimulation induces the simultaneous *O*-GlcNAc modification and Akt phosphorylations in neuroblastoma cells. Our result also indicates that improvement of hyperinsulinemia relates to the reduced level of *O*-GlcNAc modification of Akt *in vivo*, though it remains unclear whether directly or indirectly KD feeding controls the *O*-GlcNAc modification of Akt. It is expected to elucidate the mechanisms how hyperglycemia promotes the *O*-GlcNAc modification of Akt *in vivo* and utilize KD feeding for the treatment of the pathologies involving *O*-GlcNAc modified Akt in near future.

In conclusion, the established mouse model is useful in evaluating the *in vivo* dynamics of *O*-GlcNAc modification that is associated with glycemic status. This study also revealed that global *O*-GlcNAc levels in tissue proteins were strictly maintained at a constant level, in spite of their glycemic status, whereas the expression levels of certain *O*-GlcNAc-modified proteins responded to the glycemic status. We propose that the *O*-GlcNAc-modified proteins that respond to glycemic status will be a prospective index for nutritional therapy for hyperglycemia-associated diseases.

Acknowledgments This work was supported by JSPS KAKENHI (22700780 and 24700895) and by a Sasakawa Scientific Research Grant from The Japan Science Society.

References

1. Hart, G.W., Housley, M.P., Slawson, C.: Cycling of *O*-linked beta-*N*-acetylglucosamine on nucleocytoplasmic proteins. Nature **446**, 1017–1022 (2007)
2. Haltiwanger, R.S., Blomberg, M.A., Hart, G.W.: Glycosylation of nuclear and cytoplasmic proteins. Purification and characterization of a uridine diphospho-*N*-acetylglucosamine:polypeptide beta-*N*-acetylglucosaminyltransferase. J. Biol. Chem. **267**, 9005–9013 (1992)
3. Dong, D.L., Hart, G.W.: Purification and characterization of an *O*-GlcNAc selective *N*-acetyl-beta-D-glucosaminidase from rat spleen cytosol. J. Biol. Chem. **269**, 19321–19330 (1994)
4. Hu, P., Shimoji, S., Hart, G.W.: Site-specific interplay between *O*-GlcNAcylation and phosphorylation in cellular regulation. FEBS Lett. **584**, 2526–2538 (2010)
5. Butkinaree, C., Park, K., Hart, G.W.: *O*-linked beta-*N*-acetylglucosamine (*O*-GlcNAc): extensive crosstalk with phosphorylation to regulate signaling and transcription in response to nutrients and stress. Biochim. Biophys. Acta **1800**, 96–106 (2010)
6. Copeland, R.J., Bullen, J.W., Hart, G.W.: Cross-talk between GlcNAcylation and phosphorylation: roles in insulin resistance and glucose toxicity. Am. J. Physiol. Endocrinol. Metab. **295**, E17–E28 (2008)
7. Dias, W.B., Hart, G.W.: *O*-GlcNAc modification in diabetes and Alzheimer's disease. Mol. Biosyst. **3**, 766–772 (2007)
8. Yang, X., Ongusaha, P.P., Miles, P.D., Havstad, J.C., Zhang, F., So, W.V., Kudlow, J.E., Michell, R.H., Olefsky, J.M., Field, S.J., Evans, R.M.: Phosphoinositide signaling links *O*-GlcNAc transferase to insulin resistance. Nature **451**, 964–969 (2008)
9. Dentin, R., Hedrick, S., Xie, J., Yates 3rd, J., Montminy, M.: Hepatic glucose sensing *via* the CREB coactivator CRTC2. Science **319**, 1402–1405 (2008)
10. Vosseller, K., Wells, L., Lane, M.D., Hart, G.W.: Elevated nucleocytoplasmic glycosylation by *O*-GlcNAc results in insulin resistance associated with defects in Akt activation in 3T3-L1 adipocytes. Proc. Natl. Acad. Sci. U. S. A. **99**, 5313–5318 (2002)
11. Taylor, R.P., Parker, G.J., Hazel, M.W., Soesanto, Y., Fuller, W., Yazzie, M.J., McClain, D.A.: Glucose deprivation stimulates *O*-GlcNAc modification of proteins through up-regulation of *O*-linked *N*-acetylglucosaminyltransferase. J. Biol. Chem. **283**, 6050–6057 (2008)
12. Cheung, W.D., Hart, G.W.: AMP-activated protein kinase and p38 MAPK activate *O*-GlcNAcylation of neuronal proteins during glucose deprivation. J. Biol. Chem. **283**, 13009–13020 (2008)
13. Taylor, R.P., Geisler, T.S., Chambers, J.H., McClain, D.A.: Up-regulation of *O*-GlcNAc transferase with glucose deprivation in HepG2 cells is mediated by decreased hexosamine pathway flux. J. Biol. Chem. **284**, 3425–3432 (2009)
14. Kang, J.G., Park, S.Y., Ji, S., Jang, I., Park, S., Kim, H.S., Kim, S.M., Yook, J.I., Park, Y.I., Roth, J., Cho, J.W.: *O*-GlcNAc protein modification in cancer cells increases in response to glucose deprivation through glycogen degradation. J. Biol. Chem. **284**, 34777–34784 (2009)
15. Park, K., Saudek, C.D., Hart, G.W.: Increased expression of beta-*N*-acetylglucosaminidase in erythrocytes from individuals with prediabetes and diabetes. Diabetes **59**, 1845–1850 (2010)
16. Liu, K., Paterson, A.J., Chin, E., Kudlow, J.E.: Glucose stimulates protein modification by *O*-linked GlcNAc in pancreatic beta cells: linkage of *O*-linked GlcNAc to beta cell death. Proc. Natl. Acad. Sci. U. S. A. **97**, 2820–2825 (2000)
17. Housley, M.P., Rodgers, J.T., Udeshi, N.D., Kelly, T.J., Shabanowitz, J., Hunt, D.F., Puigserver, P., Hart, G.W.: *O*-GlcNAc regulates FoxO activation in response to glucose. J. Biol. Chem. **283**, 16283–16292 (2008)
18. Levi, I., Segev, Y., Priel, E.: Type 1 diabetes affects topoisomerase I activity and GlcNAcylation in rat organs: kidney liver and pancreas. Glycobiology **22**, 704–713 (2012)
19. Roos, M.D., Xie, W., Su, K., Clark, J.A., Yang, X., Chin, E., Paterson, A.J., Kudlow, J.E.: Streptozotocin, an analog of *N*-acetylglucosamine, blocks the removal of *O*-GlcNAc from intracellular proteins. Proc. Assoc. Am. Physicians **110**, 422–432 (1998)
20. Hanover, J.A., Lai, Z., Lee, G., Lubas, W.A., Sato, S.M.: Elevated *O*-linked *N*-acetylglucosamine metabolism in pancreatic beta-cells. Arch. Biochem. Biophys. **362**, 38–45 (1999)
21. Okuda, T., Morita, N.: A very low carbohydrate ketogenic diet prevents the progression of hepatic steatosis caused by hyperglycemia in a juvenile obese mouse model. Nutr. Diabetes **2**, e50 (2012)
22. Coleman, D.L., Hummel, K.P.: The influence of genetic background on the expression of the obese (*Ob*) gene in the mouse. Diabetologia **9**, 287–293 (1973)
23. Badman, M.K., Kennedy, A.R., Adams, A.C., Pissios, P., Maratos-Flier, E.: A very low carbohydrate ketogenic diet improves glucose tolerance in *ob/ob* mice independent of weight loss. Am. J. Physiol. Endocrinol. Metab. **297**, E1197–E1204 (2009)
24. Kennedy, A.R., Pissios, P., Out, H., Roberson, R., Xue, B., Asakura, K., Furukawa, N., Marino, F.E., Liu, F.F., Kahn, B.B., Libermann, T.A., Maratos-Flier, E.: A high-fat, ketogenic diet induces a unique metabolic state in mice. Am. J. Physiol. Endocrinol. Metab. **292**, E1724–E1739 (2007)
25. Comer, F.I., Vosseller, K., Wells, L., Accavitti, M.A., Hart, G.W.: Characterization of a mouse monoclonal antibody specific for *O*-linked *N*-acetylglucosamine. Anal. Biochem. **293**, 169–177 (2001)
26. Teo, C.F., Ingale, S., Wolfert, M.A., Elsayed, G.A., Nöt, L.G., Chatham, J.C., Wells, L., Boons, G.J.: Glycopeptide-specific monoclonal antibodies suggest new roles for *O*-GlcNAc. Nat. Chem. Biol. **6**, 338–343 (2010)
27. Lazarus, B.D., Love, D.C., Hanover, J.A.: Recombinant *O*-GlcNAc transferase isoforms: identification of *O*-GlcNAcase, yes tyrosine kinase, and tau as isoform-specific substrates. Glycobiology **16**, 415–421 (2006)
28. Hanover, J.A., Yu, S., Lubas, W.B., Shin, S.H., Ragano-Caracciola, M., Kochran, J., Love, D.C.: Mitochondrial and nucleocytoplasmic isoforms of *O*-linked GlcNAc transferase encoded by a single mammalian gene. Arch. Biochem. Biophys. **409**, 287–297 (2003)
29. Liu, Y., Li, X., Yu, Y., Shi, J., Liang, Z., Run, X., Li, Y., Dai, C.L., Grundke-Iqbal, I., Iqbal, K., Liu, F., Gong, C.X.: Developmental regulation of protein *O*-GlcNAcylation, *O*-GlcNAc transferase, and *O*-GlcNAcase in mammalian brain. PLoS One **7**, e43724 (2012)
30. Macauley, M.S., Vocadlo, D.J.: Enzymatic characterization and inhibition of the nuclear variant of human *O*-GlcNAcase. Carbohydr. Res. **344**, 1079–1084 (2009)
31. Snow, C.M., Senior, A., Gerace, L.: Monoclonal antibodies identify a group of nuclear pore complex glycoproteins. J. Cell. Biol. **104**, 1143–1156 (1987)
32. Holt, G.D., Snow, C.M., Senior, A., Haltiwanger, R.S., Gerace, L., Hart, G.W.: Nuclear pore complex glycoproteins contain cytoplasmically disposed *O*-linked *N*-acetylglucosamine. J. Cell. Biol. **104**, 1157–1164 (1987)
33. Manning, B.D., Cantley, L.C.: AKT/PKB signaling: navigating downstream. Cell **129**, 1261–1274 (2007)
34. Wang, S., Huang, X., Sun, D., Xin, X., Pan, Q., Peng, S., Liang, Z., Luo, C., Yang, Y., Jiang, H., Huang, M., Chai, W., Ding, J., Geng, M.: Extensive crosstalk between *O*-GlcNAcylation and phosphorylation regulates Akt signaling. PLoS One **7**, e37427 (2012)
35. Wang, Z., Park, K., Comer, F., Hsieh-Wilson, L.C., Saudek, C.D., Hart, G.W.: Site-specific GlcNAcylation of human erythrocyte proteins: potential biomarker(s) for diabetes. Diabetes **58**, 309–317 (2009)
36. Gandy, J.C., Rountree, A.E., Bijur, G.N.: Akt1 is dynamically modified with *O*-GlcNAc following treatments with PUGNAc and insulin-like growth factor-1. FEBS Lett. **580**, 3051–3058 (2006)
37. Lazarus, B.D., Love, D.C., Hanover, J.A.: *O*-GlcNAc cycling: implications for neurodegenerative disorders. Int. J. Biochem. Cell Biol. **41**, 2134–2146 (2009)